A FAILURE CRITERION FOR SUBASSEMBLY FUEL ELEMENTS SUBJECTED TO A PRESSURE PULSE LOADING*

R.C. HIBBELER, P.Y. WANG

Reactor Analysis and Safety Division, Argonne National Laboratory, Argonne, Illinois 60439, U.S.A.

SUMMARY

The potential for fuel element failure propagation is of concern for both the operation and safety of nuclear reactors. A sudden failure of one fuel element may potentially lead to a cascading failure of adjacent elements, which may ultimately threaten the integrity of the subassembly. The nature of this failure may be a sudden clad breach caused by internal pressure, and consequently, a shock wave may be formed.

In assessing the damage which may be caused by the shock wave, it is assumed that the fuel element fails near the plenum region, since the combination of temperature and radiation effects within this region are severe. Furthermore, the dynamic effects are anticipated to be more severe in this region since fission gas escape is more rapid following rupture, and the adjacent fuel elements have low inertia characteristics. Essentially, the problem is formulated on the basis of establishing a failure criterion for a thin cylindrical shell sustaining an internal pressure and subjected to a side-on blast load. The transient loading considered here is of the form $p = p_0 \cos\theta\, e^{-\alpha t}(-\pi/2 \leqslant \theta \leqslant \pi/2)$, however, other pressure loadings may also be considered.

Experiments show that thin tubes, subjected to side-on blast loads, buckle by forming a collapse-hinge at the point of maximum moment. Since there is a striking similarity between the collapse-hinge formed by blast and that formed by a statically applied bending moment, it is suggested that bending of the cylinder generates the weakness which results in collapse-hinge failure of the cylinder. Due to bending, the original (circular) cross-section ovalizes, which gives rise to nonbifurcation instability of the cylinder as a whole. The critical moment (M_{cr}) and the moment curvature relationship, which accommodates ovalization, can be found in the literature. Using this relationship, a dynamic analysis is presented using an energy approach, whereby a static deflection shape of the shell's centerline is multiplied by suitable time-varying functions to obtain the bending moment in the shell. When this moment equals M_{cr}, failure is said to occur at the shell's midpoint. To complete this investigation, a contact stress analysis at the wire wrap support is also included.

The validity of the analysis is demonstrated by comparing it with experimental data. Using the theory, many calculations are performed in an effort to study how the blast characteristics are related to collapse-hinge failure, fuel-pin geometry, and material properties. Parameters used in this study are typical for fuel elements used in current LMFBR designs.

* This work was performed under the auspices of the U.S. Atomic Energy Commission.

1. Introduction

The following presentation is concerned with the analysis of fuel element failure propagation caused by a sudden fuel element rupture. In particular, if the pressure pulse created by a rupture is large enough, two events causing damage must be investigated. First, the pulse may severely deform the neighboring pins and, as a consequence, the coolant flow may be restricted. The extent of this localized deformation to adjacent pins is investigated using a bending analysis. Secondly, the pressure pulse may cause localized deformation to a neighboring pin, enough to cause a similar rupture and hence propagate the failure. For LMFBR reactors, this localized deformation occurs at wire wrap points of contact between adjacent pins. Using a dynamic-plastic analysis, stress and deformation effects developed at the wire wrap points of contact are considered.

2. Localized Collapse Due to Buckling

2.1 Analysis

Experimental work originally performed by Blazer [1] indicates that a static collapse-hinge form of buckling occurs in a long thin cylinder, when the cylinder is subjected to beam bending. Since there is a striking similarity between the collapse-hinge formed by blast and that formed by a statically applied bending moment, it has been suggested by Woodward and Anderson [2] that bending of the cylinder generates a weakness which results in a collapse-hinge failure of the cylinder. Essentially, when the cylinder deforms, the original (circular) cross-section ovalizes which gives rise to nonbifurcation instability of the cylinder as a whole. Since the ovalization effect of the cross-section prevents the cylinder from acting like a beam (having a solid cross-section), Wood [3] has modified the conventional beam moment-curvature relationship to accommodate ovalization. In particular, he has shown that if the cylinder is assumed long and is subjected to an internal pressure P and an applied bending moment M, Figure 1, the centerline curvature may be related to the applied moment by the equation

$$M = -EI\left[\frac{1}{\rho} - K_1\left(\frac{1}{\rho}\right)^3\right] \tag{1}$$

where

$$K_1 = \frac{3}{2}\,\frac{\dfrac{a^4}{t^2}(1-\nu^2)}{\left[1 + \dfrac{4Pa^3(1-\nu^2)}{Et^3}\right]} \quad \text{and} \quad I = \pi a^3 t$$

In this equation E and ν are Young's modulus and Poisson's ratio, respectively. The maximum or collapse moment occurs when $\frac{dM}{d(1/\rho)} = 0$. This yields

$$M_{cr} = \frac{2tEI}{9a^2}\sqrt{\frac{2\left[1 + 4\,\dfrac{Pa^3}{Et^3}(1-\nu^2)\right]}{(1-\nu^2)}} \tag{2}$$

Displacement components measured relative to the centerline of the shell have also been obtained by Wood. These expressions may be written as

$$v_o = \frac{1}{2}K_2\left(\frac{1}{\rho}\right)^2 \sin 2\theta \tag{3}$$

and

$$w_o = -K_3 + K_2\left(\frac{1}{\rho}\right)^2 \cos 2\theta \tag{4}$$

where

$$K_2 = \frac{a^3(1-\nu^2)\left[1 + \left(\frac{2-\nu}{2}\right)\left(\frac{Pa}{Et}\right)\right]}{\left[\left(\frac{t}{a}\right)^2 + 4(1-\nu^2)\left(\frac{Pa}{Et}\right)\right]}$$

and

$$K_3 = \left(\frac{2-\nu}{2}\right)\frac{Pa^2}{Et}$$

The higher order terms in these expressions have been neglected since they are small compared to other terms in the equations for values of t/a and P which are appropriate for fuel elements. Furthermore, a deflection term proportional to curvature has also been neglected in the above expressions. This term represents the St. Venant displacement plus rigid body motion which is small compared to the other terms.

The deflection of the centerline of the shell is represented by $Z(x,t)$. Hence, the displacement components at any instant can be written as

$$v = Z \sin\theta + v_o \tag{5}$$

and

$$w = Z \cos\theta + w_o \tag{6}$$

The centerline deflection is related to the curvature by

$$\frac{1}{\rho} = \frac{d^2Z}{dx^2} - \frac{3}{2}\frac{d^2Z}{dx^2}\left(\frac{dZ}{dx}\right)^2 \tag{7}$$

Using eqs. (3) - (7), the deformed state $\vec{u}$ can be expressed in vector form as

$$\vec{u} = \left\{K_2\left(\frac{d^2Z}{dx^2} - 3\left(\frac{d^2Z}{dx^2}\right)^2\left(\frac{dZ}{dx}\right)^2\right)\sin^3\theta + K_3 \sin\theta\right\}\hat{j} + \tag{8}$$

$$+ \left\{Z + K_2\left(\frac{d^2Z}{dx^2} - 3\left(\frac{d^2Z}{dx^2}\right)^2\left(\frac{dZ}{dx}\right)^2\right)\cos^3\theta - K_3\cos\theta\right\}\hat{k}$$

where $\hat{j}$ and $\hat{k}$ are directed along the y and z axis.

The principle of virtual work will be used for the solution. This principle states that in a dynamically deformed state, the change in the internal strain energy of the cylinder is equal to the change of work caused by the surface, body, and inertia forces when the cylinder is subjected to a variation in its deformation. Since the dynamic effects caused by fission gas escape during rupture are most severe within the plenum region of the fuel element, the body forces can be neglected. Hence,

$$\delta U = \int_S \vec{F} \cdot \delta\vec{u}\, dS - \int_V \gamma_V \ddot{\vec{u}} \cdot \delta\vec{u}\, dV \tag{9}$$

where γ_V represents the mass density of the material.

The internal strain energy δU is computed from bending, as in beam theory. Using eq. (1) neglecting terms greater than the fourth order

$$U = \frac{EI}{2}\int_0^L \left(\left(\frac{1}{\rho}\right)^2 - 2K_1\left(\frac{1}{\rho}\right)^4\right) dx$$

Substituting eq. (7) into this expression, computing the first variation, and simplifying,

$$\delta U = EI\int_0^L \left\{\left[\frac{d^2Z}{dx^2} - 3\frac{d^2Z}{dx^2}\left(\frac{dZ}{dx}\right)^2 - 4K_1\left(\frac{dZ}{dx}\right)^3\right]\delta\left(\frac{d^2Z}{dx^2}\right) - 3\left(\frac{d^2Z}{dx^2}\right)^2\frac{dZ}{dx}\,\delta\left(\frac{dZ}{dx}\right)\right\} dx \tag{10}$$

Since the internal pressure was not included in the computation for the internal strain energy, its effect is likewise excluded from the calculation of the external virtual work.

Only the pressure pulse causes bending of the shell. The pulse will be assumed constant over the length of the shell and to decay exponentially with time (other pressure distributions may also be used). The radial pressure p is represented here as

$$p = p_o \cos\theta \, (e^{-\alpha\tau} - e^{-\beta\tau}) \qquad -\frac{\pi}{2} \le \theta \le \frac{\pi}{2}$$
$$p = 0 \qquad \frac{\pi}{2} \le \theta \le \frac{3\pi}{2} \tag{11}$$

As shown in Figure 2, p_o represents the maximum (peak) pressure. α and β are decay parameters used to indicate the transient response of the pressure, $\beta > \alpha$.

$$\int_S \vec{F} \cdot \delta\vec{u} \, dS = \int_S p \cos\theta \, \delta Z \, dS = \frac{\pi}{2} p_o \, a(e^{-\alpha\tau} - e^{-\beta\tau}) \int_0^L \delta Z \, dx \tag{12}$$

The virtual work of the inertia forces is represented in terms of the deformation state $\vec{u}$. Taking the appropriate derivatives of eq. (8) and integrating over θ yields the following expression for the virtual work of the inertia forces

$$\int_V \left(\frac{d^2\vec{u}}{d\tau^2} \cdot \delta\vec{u}\right) dV = \gamma_L \int_0^L \left\{ \frac{d^2Z}{d\tau^2} \delta Z + \frac{5}{2} K_2^2 \frac{d^2Z}{dx^2} \left[\left(\frac{d^3Z}{dx^2 d\tau}\right)^2 + \frac{d^2Z}{dx^2}\left(\frac{d^4Z}{dx^2 d\tau^2}\right)\right] \delta\left(\frac{d^2Z}{dx^2}\right)\right\} dx \tag{13}$$

In this expression γ_L represents the mass density per unit length of shell, i.e., $\gamma_L = 2\pi t a \gamma_V$.

Since the shell is simply supported at its ends, the centerline deflection may be represented by the series expansion

$$Z(x,\tau) = \sum A_n(\tau) \sin\frac{n\pi x}{L} . \tag{14}$$

As a first approximation to the solution, only the first term of the series will be considered. (Including a third term improves the deflection accuracy by only 4%.) Substituting this into eqs. (9), (10), (12), and (13), and integrating over the length yields the following time-dependent nonlinear differential equation

$$\ddot{A}_1 \left[1 + \frac{15}{8} K_2^2 \left(\frac{\pi}{L}\right)^8 A_1^2\right] + \frac{15}{8} K_2^2 \left(\frac{\pi}{L}\right)^8 A_1 \dot{A}_1^2 + \tag{15}$$
$$+ \frac{\pi^5 E a^3 t}{\gamma_L L^4} A_1 \left[1 - 3K_1 \left(\frac{\pi}{L}\right)^4 A_1^2 - \frac{3}{2}\left(\frac{\pi}{L}\right)^2 A_1^2\right] = \frac{2p_o a(e^{-\alpha\tau} - e^{-\beta\tau})}{\gamma_L}$$

Solution of this equation yields the deformation state as a function of time τ. Since a closed form solution cannot be obtained, a numerical solution using the Runge-Kutta method is suggested.

The maximum moment is developed at the midpoint of the shell ($x = \frac{L}{2}$). Combining eqs. (1) and (7) and using the first term approximation for eq. (14), the maximum moment becomes

$$M_{max} = E\pi a^3 t \left(\frac{\pi}{L}\right)^2 A_1 \left[1 - K_1 \left(\frac{\pi}{L}\right)^4 A_1^2\right]. \tag{16}$$

Failure of the shell is said to occur if the blast load is sufficient to cause the maximum moment [eq. (16)] to equal the critical moment defined by eq. (2).

2.2 Experimental Verification

The validity of the preceding analysis is demonstrated by comparing it with experimental data compiled by Bores [4] and obtained from the explosion of a fuel pin located at the center of an EBR-II subassembly immersed in water. In this particular experiment, the

pressure pulse at the duct wall was measured as a function of time. Since the rise time was very short, the pulse is characterized by the equation $p = p_d e^{-\alpha\tau}$ where p_d = 3,150 psi (peak pressure) and α = 17,241.4 sec^{-1}. From observation, the first two concentric rings of fuel elements surrounding the central fuel pin showed evidence of collapse failure due to this loading. Beyond the second ring of the fuel elements, no damage was noticeable.

Failure as predicted from the above analysis was found to agree with the experimental observations described above. Equation (11) was used for making these predictions. The value of α was assumed to be independent of geometry and to depend solely on the characteristics of the blast. Due to the fast rise time of the pulse, the term involving β is neglected. The peak pressure p_o was computed at the radius of each concentric ring of fuel elements from the central element by assuming that following the explosion, the pressure of the expanding spherical wave front is inversely proportional to the radius of the sphere at any instant. In particular, the fuel element was assumed to be simply supported with L = 6 in. This is the distance between points of contact of the helical wire-wraps and an adjacent fuel element.

2.3 Results and Conclusions

Using the computer program RUPTURE, many calculations were performed based upon the theory in an effort to study how the blast characteristics are related to collapse-hinge failure, fuel-pin geometry, and material properties. Parameters used in this study are typical for fuel elements used in current LMFBR designs.

A parametric study of the effect of cylinder support length L on the generated collapse moment M_{max} in the cylinder reveals that dramatic increases in moment exist for support lengths less than about four inches. Beyond this, the curves approach an asymptotic value. Since the effect of finite length on ovalization of the cylinder was neglected in the analysis, it is suspected that the results predicted from this theory are invalid for support lengths $L \leq 4$ in. For typical fuel element geometries considered here, the supporting length distance L is 6 in. as mentioned previously.

The curves shown in Figure 3 illustrate how the induced moment M varies for different fuel element radii and material properties (or temperature). It can be seen that the critical moment varies in a linear fashion with radius. Furthermore, increasing the temperature enhances the possibility of failure. (Although not shown on the graph, increasing the thickness of the fuel element clad provides more stiffness for the fuel element and thereby insures against collapse-hinge failure.)

In reality, current fuel element plenums generally sustain internal pressures between 500 and 1000 psi toward the end of their lifetimes. The effect of a blast caused by these pressures has been ascertained using the present theory. Assume as an upper limit, for example, a blast having a peak pressure of p_o = 1000 psi impinges upon a neighboring LMFBR fuel element. If the transient decay $\alpha \leq 1{,}600$ sec^{-1}, it is found that possible collapse can occur. The possibility of obtaining an α having this magnitude depends upon the nature of the fuel element rupture. Existing blast data from van Erp *et al.* [5], however, proves that values of $\alpha < 4{,}500$ sec^{-1} will be quite improbable in the event of a clad rupture.

The results of the analysis, therefore, indicate that no severe damage to the adjacent clad of a fuel element can be expected from the possible rupture of a fuel element plenum provided the element is sustaining an internal pressure of about 1000 psi when it ruptures.

Upon rupture, side-on blast pressures which are greater than 1000 psi are generally not expected.

3. Localized Contact Interactions

3.1 Analysis

The possibility of pin-to-pin failure propagation will be studied on the basis of analyzing the localized stress and deformations occurring at the wire wrap. In attempting to draw some valid conclusions regarding the mechanical interactions between fuel elements, several conservative assumptions are made. The pressure pulse loading is defined by eq. (11). Again, the plenum region of the fuel element is considered since the inertia characteristics of the plenum (or hollow cylinder) are low and the gas release rate from the adjacent fuel element plenum is high. The pulse loading is applied only along a segmented length L' of the cylinder. During normal operating conditions, the fuel elements are arranged in a "tight" assembly; consequently, the supports are located at points of contact with the wire wrapping, and these supports are assumed fixed from motion. The pressure pulse will cause the most severe mechanical interaction stresses if it is located directly over the support as shown in Figure 4. In the event of a fuel element burst, it is expected that the failed fuel element will tear open longitudinally when the plenum gas is released. The extent of such ruptures has been reported in the literature [6] where it is found that no tear has exceeded 1/2 in. Due to the fast rate of gas release, the characteristics of the burst, and the proximity of the adjacent fuel element (56 ml), it is assumed that the pressure loading length L' in Figure 4 is equal to the axial length of the tear formed in the ruptured fuel element. Since $L >> L'$, this distributed load is localized over the support. The force created by the pressure pulse is transmitted to the neighboring fuel elements which are located adjacent to the ruptured fuel element, since the wire-wrapping contacts adjacent fuel elements at the same elevation. The problem to be considered for all practical purposes is, therefore, that due to a pair of equal but opposite concentrated radial loads acting on a cylinder. An empirical set of formulas developed by Roark [7] can be used to determine the elastic stress and deflection under these loads. Using these formulas, it is found that for most LMFBR geometries, the contact stress at the support remains elastic provided the crack length developed in the failed fuel element is not larger than 1/4 in. Failure analysis for cracks greater than 1/4 in. must account for the effects of plastic yielding. The upper bound on crack length is about 1/2 in. Using a conservative analysis, it will presently be shown that this upper limit in crack size is still not sufficient to cause failure.

From the geometry of the fuel element, the wire wrap pitch is small ($\sim 8.5°$) so that the contact loading is applied radially, approximately along the axis of the cylinder. Furthermore, resistance to the loading is strongly dependent upon the hoop tangential and bending stresses. It becomes reasonable to neglect the bending and membrane resistance in the axial direction of the shell, and thereby model the response behavior of a thin ring which is symmetrically loaded by two radial pulse loads. Using a dynamic analysis of a ring, developed by Owens and Symonds [8], the strain energy density stored in the material, localized at the points of contact can be computed for an exponential time varying pulse. As a conservative estimate, a pulse having a peak of 1000 psi and a decay time of 0.1 ms has been considered. Comparing the strain energy density with the maximum strain energy density which can be developed in the material for high strain rates, it is found that the

adjacent fuel element needs 3.43 times as much energy for failure than that provided by the pulse. Because of this and due to the conservative assumptions used in formulating the solution of this problem, it appears that a sudden fuel element rupture does not cause further fuel element failure propagation. Even if failure does indeed propagate to a neighboring fuel element, it would seem rather presumptuous to expect a further propagation by a similar rupture mechanism, since failure propagation would depend upon producing tears of approximately 1/4 in. to 1/2 in. in length. Recent experiments by Lauritzen [9] substantiate the fact that the failure region in the majority of the fuel elements is not even discernible with the unaided eye. Under low power magnification, these "failure zones" are characterized in most cases by a family of parallel longitudinal fractures. If localized stresses cause failure of a fuel element, it is expected that the failure will have this microscopic nature.

References

[1] L. G. Brazier, "On the Flexure of Thin Cylindrical Shells and Other 'Thin' Sections," *Proc. Roy. Soc.*, London, Series A, *116*, 104-114 (1927).

[2] J. H. Woodward, J. P. Anderson, "A Model for Collapse-Hinge Instability of Blast-Loaded Cylinders," *Developments in Theoretical and Applied Mechanics, 4*, Pergamon Press (1966).

[3] J. D. Wood, "The Flexure of a Uniformly Pressurized Circular, Cylindrical Shell," *J. Appl. Mech.*, 453-458 (Dec 1958).

[4] B. L. Boers, "Explosive Technique for Pressure Pulse Testing of Reactor Components," *Trans. Am. Nucl. Soc.*, *12*(2), 828 (1969).

[5] J. B. van Erp, et al., *Fission-Gas Release in LMFBR Fuel Subassemblies*, Argonne National Laboratory, ANL/RAS 71-19 (Apr 1971).

[6] *Material Considerations in Support of the FFTF Preliminary Safety Analysis Report*, RM-9 HEDL, Vol. 1, (Apr 1971).

[7] R. J. Roark, "The Strength and Stiffness of Cylindrical Shells under Concentrated Loading," *J. Appl. Mech.*, *2*(4), A-147 (1935).

[8] R. H. Owens and P. S. Symonds, "Plastic Deformation of a Free Ring under a Concentrated Dynamic Loading," *J. Appl. Mech.*, 523-529 (Dec 1955).

[9] T. Lauritzen, *Stress-Rupture Behavior of Austenitic Stainless Steel Tubing*, GEAP-13897 (Jan 1972).

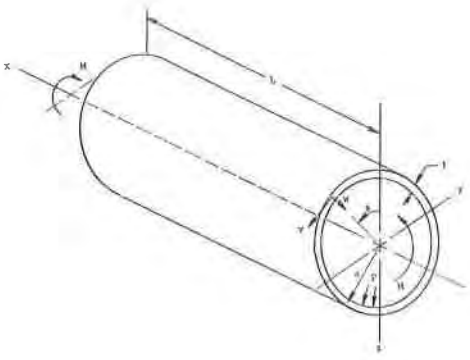

Figure 1 Shell Coordinate System and Geometry

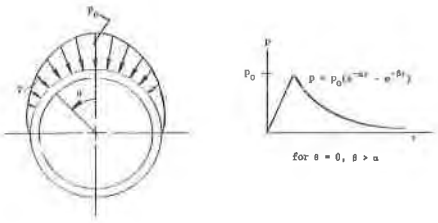

Figure 2 Impulsive Loading Distribution on Shell

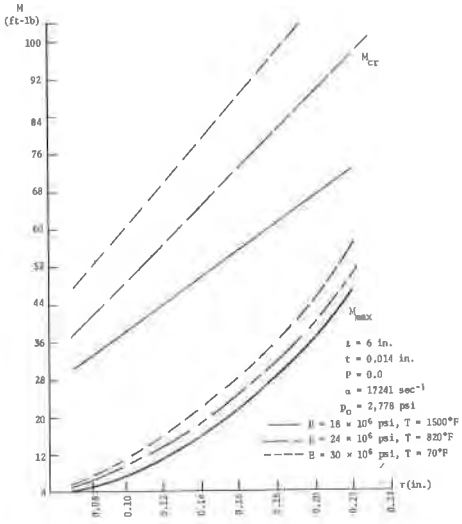

Figure 3 The Effects of Fuel-element Radius and Temperature on Moment, M

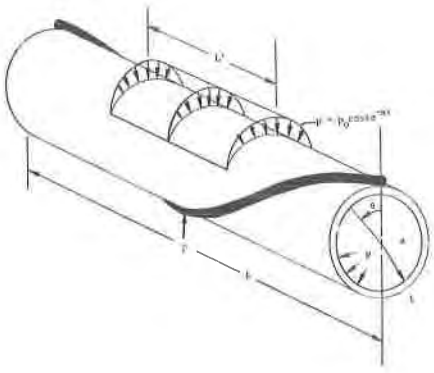

Figure 4 Loading and Geometry of Fuel Element Plenum